International Journal of Modern Physics D Vol. 11 No. 7 (2002) 963–994

Detecting gravitational waves with ground and space interferometers – with special attention to the space project ASTROD

ALBRECHT RÜEDIGER

Max-Planck-Institut für Gravitationsphysik, Albert-Einstein-Institut, Hans-Kopfermann-Str. 1, D – 85748 Garching, Germany

Received 27 May 2002

The existence of gravitational waves is the most prominent of Einstein's predictions that has not yet been directly verified. The space projects LISA and (partially) ASTROD share their goal and principle of operation with the ground-based interferometers currently under construction: the detection and measurement of gravitational waves by laser interferometry. Ground and space detection differ in their frequency ranges, and thus the detectable sources. Towards low frequencies, ground-based detection is limited by seismic noise, and yet more fundamentally by 'gravity gradient noise', thus covering the range from a few Hz to a few kHz. On five sites worldwide, detectors of armlengths from 0.3 to 4 km are nearing completion. They will progressively be put in operation in the years 2002 and 2003. Future enhanced versions are being planned, with scientific data not expected until 2008, i.e. near the launch of the space project LISA. It is only in space that detection of signals below, say, 1 Hz is possible, opening a wide window to a different class of interesting sources of gravitational waves. The project LISA consists of three spacecraft in heliocentric orbits, forming a triangle of 5 million km sides. A technology demonstrator, designed to test vital LISA technologies, is to be launched, aboard a SMART-2 mission, in 2006. The proposed mission ASTROD will, among other goals, also aim at detecting gravitational waves, at even lower frequencies than LISA. Its later start will allow it to benefit from the expertise gained with LISA.

1. Introduction

The three talks on which this paper is based dealt with a new window in astronomic observation presently being opened: the detection and measurement of gravitational waves. This is one of the great challenges to modern physics. Although predicted by Einstein in 1916, a direct observation of these waves has yet to be accomplished.

Great hopes of such detection lie in the ground-based laser-interferometric detectors currently nearing completion. These ground-based detectors are sensitive in the 'audio' frequencies of a few Hz up to a few kHz. Perhaps even more promising are the space-borne interferometers, where we will mainly have to think of the joint ESA-NASA project LISA (Laser Interferometer Space Antenna), which would cover the frequency range from about 10^{-4} Hz to 1 Hz. A welcome extension of this frequency range, perhaps down to less than 10^{-5} Hz, could come from the mission ASTROD, to which this Symposium is dedicated.

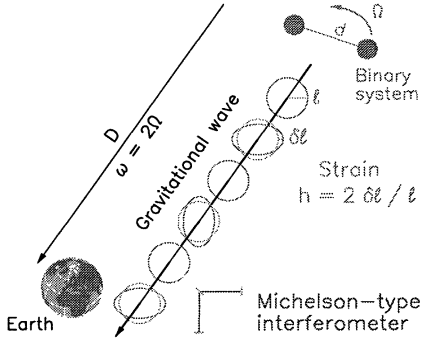

Fig. 1. Generation and propagation of a gravitational wave emitted by a binary system.

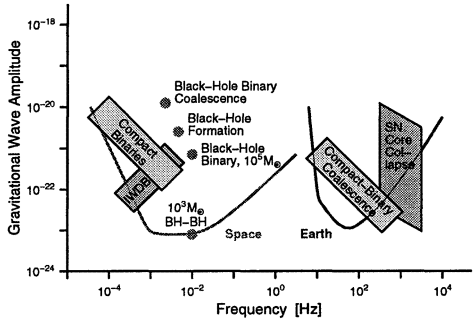

Fig. 2. Some sources of gravitational waves, with sensitivities of *Earth* and *Space* detectors.

Gravitational waves (GW) share their elusiveness with neutrinos: they have very little interaction with the measuring device, which is why these gravitational waves have not yet directly been detected. But that same feature also is a great advantage: due to their exceedingly low interaction with matter, gravitational waves can give us an unobstructed view into astrophysical and cosmological events that will forever be obscured in the electromagnetic window.

The price we have to pay is that, in order to detect and measure these gravitational waves, we will require the most advanced technologies in optics, lasers, and interferometry.

Efforts to observe these gravitational waves with ground-based interferometers have gone into their final phase of commissioning, and next-generation detectors are already in the discussion. Furthermore, an international collaboration on placing a huge interferometer, LISA, into an interplanetary orbit is close to reaching final approval. A space project ASTROD (Astrodynamical Space Test of Relativity using Optical Devices), designed mainly for the measurement of relativistic effects caused by the solar mass, will also attempt to measure gravitational waves, in a frequency range even lower than that of LISA.

We will briefly discuss the characteristics of large GW detectors being built right now, many already close to commissioning. In this talk we will learn how the detectors on ground and in space differ, where aims and technologies overlap, and what can scientifically be gained from the complementarity of these researches.

2. Gravitational waves

In two publications[1,2], Albert Einstein has predicted the existence and estimated the strength of gravitational waves. They are a direct outcome of his Theory of General Relativity, but a necessary consequence of *all* theories with finite velocity of interaction. Good introductions to the nature of gravitational waves, and on the possibilities of measuring them are given in two papers by Kip Thorne[3,4].

It can be shown that gravitational waves of measurable strengths are emitted

only when large cosmic masses undergo strong accelerations, for instance – as shown schematically in Figure 1 – in the orbits of a (close) binary system. The effect of such a gravitational wave is an apparent strain in space, transverse to the direction of propagation, that makes distances ℓ between test bodies shrink and expand by small amounts $\delta\ell$, at twice the orbital frequency: $\omega = 2\Omega$. The strength of the gravitational wave, its "amplitude", is generally expressed by $h = 2\,\delta\ell/\ell$. An interferometer of the Michelson type, typically consisting of two orthogonal arms, is an ideal instrument to register such differential strains in space.

But what appears so straighforward turns out to be an almost insurmountable problem. It lies in the magnitude, or rather: the smallness, of the effect.

2.1. *Strength of gravitational waves*

With a linearized approximation, the so-called "quadrupole formula", the strength of the gravitational wave emitted by a mass quadrupole can be estimated, and for a binary with components of masses M_1 and M_2, or their respective Schwarzschild radii R_1, R_2, the strain h to be expected is of the order

$$h \approx \frac{R_1 R_2}{d\,D} \tag{1}$$

where d and D are the distances between the partners and from binary to the observer (see Figure 1). For neutron stars, and even better for black holes, the distance d can be of the order of a Schwarzschild radius, which then would further simplify the estimate.

From such an in-spiral of a neutron star binary out at the Virgo cluster (a cluster of about 2000 galaxies, $D \sim 10\,\mathrm{Mpc}$ away), we could expect a strain of something like $h \approx 10^{-22}$. Similar (or even lower) strengths might be expected from supernovae out at Virgo cluster distances. That we insert such a large distance as the Virgo cluster is to have a reasonable rate of a few events per year. Inside a single galaxy (as ours), we would not count more than a few supernovae per century.

So all we have to do is to measure – in a Michelson interferometer of kilometer dimensions – path changes in the order of $10^{-19}\,\mathrm{m}$. *Hopeless?* The sensitivities obtained with prototypes of ground-based interferometers bear evidence that it is within reach.

And yet, despite the smallness of the interaction, gravitational waves are by no means a "weak" phenomenon. On the contrary, they are linked with cosmic events of high energy transfers. Some examples show this clearly.

The *binary system* containing the Hulse-Taylor pulsar PSR 1913+16, much publicised through the 1993 Nobel prize, loses its orbital energy primarily through the emission of gravitational radiation; no other loss mechanism comes anywhere near it. It is a very convincing, albeit indirect, evidence of the existence of gravitational waves, as observation and prediction agree to much better than 1 %.

A *supernova*, on the other hand, in its final milliseconds of collapse, emits more power than the (visible) luminescence of all the stars of the universe combined.

Although most of this is in neutrinos, an appreciable part is also emitted in gravitational waves, from the rebound of the core.

The formation, and the interaction, of massive and supermassive black holes, believed to be at the centers of most galaxies, are perhaps the most violent events in the Universe, and the gravitational waves emitted by them will be our best chance to investigate the physics involved. This type of gravitational waves will come in a frequency region well below 1 Hz, and only space projects will be able to detect them. Of these projects, the plans for the ESA-NASA mission LISA have reached maturity, and a project ASTROD is in the early stages of a study phase.

2.2. *What makes gravitational waves so special ?*

Let us see what can be learned about the nature of gravitational waves in a comparison with electromagnetic waves. What they do have in *common* is the velocity of propagation: the speed of light c. And also, from conservation of energy, the decline in amplitude with the inverse of the distance travelled, see Eq. (1).

But there are fundamental *differences* between electrical and gravitational forces. While in electromagnetism we have two opposite charges, gravity is governed by mass having only one sign (and the gravitational forces being attractive).

The most basic radiation mode in electromagnetism is thus the dipole, in the case of gravitation, however, the quadrupole. One result of that is that the frequency ω of the emitted gravitational wave is twice the orbital frequency Ω, as an identical mass distribution is already reached after half an orbital period. The quadrupole radiation also implies a different polarization pattern: In electromagnetism, the two polarizations are off by 90°, in gravitational waves by 45°. This will mean that the Michelson interferometer indicated in Figure 1 is optimized for a wave as the one shown (+), whereas it would be insensitive to a wave 45° off (×).

Electrical attraction between, say, electron and proton is nearly 10^{40} times bigger than the gravitational one. But this does not justify considering gravity negligibly weak. The strong electrical attraction leads to mutual saturation, and thus globally to a cancelling: there are practically no large agglomerations of free charges in nature. What we observe in electromagnetic radiation are mainly the non-coherent motions of individual charges on microscopic scales.

For gravitation, on the other hand, we have masses of only one sign, governed by attraction. Thus in gravitational radiation we see collective, coherent motions of large masses. And huge masses are required to counteract the "small" value of the gravitational constant.

The electromagnetic radiation is easily obscured and absorbed by matter between source and observer; not so the gravitational waves: their interaction with matter is extremely weak, it reaches us effectively unblemished by any obstacles.

This is the great advantage: gravitational waves allow us to observe events that remain hidden "in the light" of electromagnetic radiation. Thus completely different types of information, and new information in astronomy, astrophysics, fundamental physics can be reaped.

2.3. *Complementarity of ground and space observation*

Figure 2 shows some typical sources of gravitational radiation. They range in frequency over a vast spectrum, from the kHz region of supernovae and final mergers of compact binary stars down to mHz events due to formation and coalescence of supermassive black holes. Indicated are sources in two clearly separated regimes: events in the range from, say, 5 Hz to several kHz (and only these will be detectable with terrestrial antennas), and a low-frequency regime, 10^{-5} to 1 Hz, accessible only with a space project such as LISA. In the following sections we will see how the sensitivity profiles of the detectors come about. No detector covering the whole spectrum shown could be devised.

Clearly, one would not want to miss the information of either of these two (rather disjoint) frequency regions. The upper band ("Earth"), with supernovae and compact binary coalescence, can give us information about relativistic effects and equations of state of highly condensed matter, in highly relativistic environments. Binary inspiral is an event type than can be calculated to high post-newtonian order, as shown, e.g., by Buonanno and Damour[5]. This will allow tracing the signal, possibly even by a single detector, until the final merger, a much less predictable phase. The ensuing phase of a ring-down of the combined core does again lend itself to an approximate calculation, and thus to an experimental verification. Chances for detection are reasonably good, but not by wide margins.

The events to be detected by the space projects LISA and possibly ASTROD, on the other hand, may have extremely high signal-to-noise ratios, and failure to find them would shatter the very foundations of our present understanding of the universe. The strongest signals will come from events involving (super-)massive black holes, their formation as well when galaxies with their BH cores collide. But also the (quasi-continuous) signals from neutron-star and black-hole binaries are among the events to be detected ('Compact Binaries' in Figure 2). Interacting white dwarf binaries inside our galaxy ('IWDB' in Figure 2) may turn out to be so numerous that they cannot all be resolved as individual events. Catastrophic events such as the Gamma-ray bursts are not yet well enough understood to estimate their emission of gravitational waves, but there is a potential of great usefulness of GW detectors mainly at low frequencies. The aim of the proposed space project ASTROD is to extend this frequency range even further, to frequencies below 10^{-5} Hz.

The combined observation with electromagnetic and gravitational waves could lead to a deeper understanding of the violent cosmic events in the far reaches of the universe[6].

3. Ground-based interferometers

The underlying concept of all ground-based laser detectors is the Michelson interferometer (see schematic in Figure 3), in which an incoming laser beam is divided into two beams travelling along different (perpendicular) arms. On their return, these two beams are recombined, and their interference (measured with a photodi-

ode PD) will depend on the difference in the gravitational wave effects that the two beams have experienced. A gravitational wave propagating normal to the plane of the interferometer would give rise to a path difference δL between the two arms of

$$\delta L = h_+ \cdot L \cdot \frac{\sin(\pi f \tau)}{\pi f \tau} = h_+ \cdot L \cdot \frac{\sin(\pi L/\Lambda)}{\pi L/\Lambda} \,. \tag{2}$$

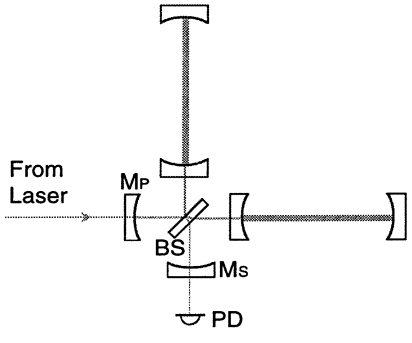

Fig. 3. Advanced Michelson interferometer with Fabry-Perots in the arms and extra mirrors M_P, M_S for power and signal recycling.

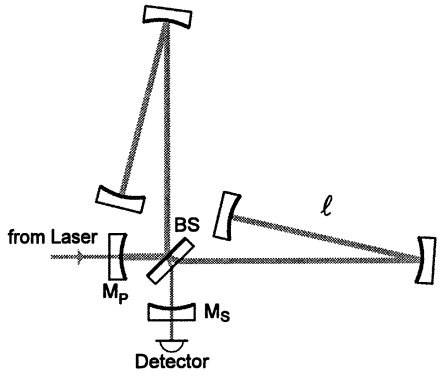

Fig. 4. The DL4 configuration with dual recycling to be used in GEO 600.

The changes δL in optical path become the larger the longer the optical paths L are made, optimally about half the wavelength Λ of the gravitational wave: e.g. to a seemingly unrealistic 150 km for a 1 kHz signal. Schemes were devised to make the optical path L significantly longer than the geometrical arm length ℓ, which is limited on Earth to only a few km. One way is to use 'optical delay lines' in the arms, the beam bouncing back and forth between two concave mirrors (a modest version of this is shown in Figure 4). The other scheme is to use Fabry-Perot cavities (Figure 3), again with the aim of increasing the interaction time of the light beam with the gravitational wave. For GW frequencies beyond the inverse of the storage time τ, the response of the interferometer will, however, roll off with frequency, as $1/f\tau$.

3.1. *The detector prototypes*

It is a fortunate feature that on our way to the large-scale detectors we were able to go through generations of ever-improving prototypes. It was only with their positive results that the proposals for large-scale detectors received sufficient credibilty.

After pioneering work by Rai Weiss[7] at MIT (1972), other groups at Munich/Garching, at Glasgow, then Caltech, Paris/Orsay, Pisa, and later in Japan and Australia, also entered the scene. Their prototypes range from a few meters up to 30, 40, and even 100 m. They all use an optical scheme modelled after the

Michelson interferometer. An alternative detection scheme, a Sagnac configuration, is being investigated at Stanford.

Based on the idea of Weiss, Garching had also adopted the scheme of the optical delay-line. The advantage was a very rapid attainment of sensitivities that were limited only by shot noise[8], by gradually reducing newly discovered noise mechanisms. It was only in the later 1990's that the (technologically more challenging) prototypes with Fabry-Perot cavities reached similar, meanwhile even better, sensitivities.

Even though some of these prototypes reached the sensitivities of cryogenic resonant-mass antennas, they were never meant to be used as detectors, but rather as test-beds for verifying new schemes and configurations devised to overcome otherwise limiting noise effects.

The "phase noise" reduction achieved in these prototypes approaches that required in full-fledged *terrestrial* interferometers, and it is by many orders of magnitude better than required (at low frequencies) for a *space mission.*

3.2. *The large-scale projects*

Table 1 gives an impression of the wide international scope of the interferometer efforts, listed according to size of detector. All of the large-scale projects will use low-noise Nd:YAG lasers ($\lambda = 1.064\,\mu$m), pumped with laser diodes for high overall efficiency. A wealth of experience has accumulated on highly stable and efficient lasers, and also the space mission will profit from that. More details about the laser source in subsection 4.1.

Table 1. Current and future projects of ground-based GW detectors

Country:	**USA**	**FRA ITA**	**GER GBR**	**JPN**
Institute:	MIT, Caltech	CNRS INFN	AEI Glasgow	NAO, U-Tokyo, ICRR

Large Interferometric Detectors: the current generation

Project name:	**LIGO**	**VIRGO**	**GEO 600**	**TAMA 300**
Arm length ℓ:	4 km 2 km 4 km	3 km	600 m	300 m
Site (State)	Hanford Livingston (WA) (LA)	Pisa ITA	Hannover GER	Mitaka JPN

Large Interferometric Detectors: the future generation

Planning (start):	1995	1999	1998
Arm length ℓ:	4 km 4 km	3 km	3 km
Site (State)	Hanford Livingston (WA) (LA)	EUROPE	Kamioka JPN
Project name:	**Advanced LIGO**	**EURO**	**LCGT**
special features:	active isolation, suspension, RSE	high seismic rejection; cryogenic, diffractive optics, tunable	cryogenic, underground

LIGO The largest is the US project named LIGO[9,10]. It comprises *two* facilities at two widely separated sites, in the states of Washington and Louisiana. Both will house a 4 km interferometer, Hanford an additional 2 km one. At both sites construction has long been completed, installation of the optics in the vacuum enclosures is done, and locking of the interferometers has now become routine. These three interferometers are designed for coincidence operation, allowing autonomous measurements inside the US project LIGO.

VIRGO Next in size (3 km) is the French-Italian project VIRGO[11], being built near Pisa, Italy. An elaborate seismic isolation system, with six-stage pendulums (see Section 4.4), will allow measurement down to GW frequencies of 10 Hz or even below, but still no overlap with the space interferometer LISA. Currently, a short-arm interferometer, with all mirrors inside the central building, is being used for performance testing.

GEO 600 For the detector of the British-German collaboration, GEO 600 [12,13], with a de-scoped length of 600 m, construction and installation of the optics in the vacuum system are finished, and locking of the full power-recycled Michelson is routinely achieved. GEO 600 will employ the advanced optical technique of "signal recycling", SR [14,15] to make up for the shorter arms. This interferometric scheme, or its counterpart "resonant sideband extraction", RSE [16], will later be transferred to the upgrades of LIGO and to the planned Australian detector.

TAMA 300 In Japan, on a site at the National Astronomical Observatory in Tokyo, construction, vacuum system, and optics installation of the detector called TAMA 300[17] with 300 m armlength are completed, and several data runs of the Michelson have been successful. A recent run with a total of 1000 hours exhibited encouragingly long in-lock duty cycles[18]. The sensitivity-enhancing scheme of power recycling will have, however, yet to be added. Separate tests with power recycling appeared promising. TAMA is, just as LIGO and VIRGO, equipped with standard Fabry-Perot cavities in the arms.

ACIGA Australia (not included in table) also had to cut back from earlier plans of a 3 km detector, due to lack of funding. Currently a 80 m prototype detector is being built near Perth, Western Australia, with the aim of investigating new interferometry configurations[19], follow-ons to the GEO schemes of signal recycling and/or RSE. The design and the site will allow later extension to 3 km.

3.3. *International collaboration*

It is fortunate that these projects are rather well in synchronism. First scientific operation can be expected around the years 2002/03. For the received signal to be meaningful, coincident recordings from at least two detectors at well-separated sites are essential. A minimum of three detectors (at three different sites) is required to locate the position of the source, and there is general agreement that only with at least four detectors can we speak of a veritable gravitational wave *astronomy*, based on a close collaboration in the exchange and analysis of the experimental data.

3.4. *First common data run (Note added in proof)*

At the turn of the year 2001/2002, a common data run between all three LIGO detectors and GEO 600 was undertaken, consisting of 17 days of mostly uninterrupted operation. This common effort can be considered quite a success.

It exhibited reasonable duty cycles of the interferometers being locked, in the GEO detector being improved considerably (up to better than 95 %) "on the fly", by upgrading the automatic mirror alignment. GEO was, however, not yet equipped with the 'signal-recycling' mirror, so not yet in its final high-sensitivity implementation.

With the detectors not yet being at the intended sensitivity level, the aim was not a search for gravitational waves, but rather to rehearse the activities of data acquisition and, then, also of data analysis. The analysis of the data, just underway, can give further clues on the 'healthiness' of the interferometers.

A second such data run between LIGO and GEO 600 is planned for the period of 23 August to 7 September, 2002, with improved noise suppression.

4. Noise and sensitivity

The measurement of gravitational wave signals is a constant struggle against the many types of noise entering the detectors. These noise sources have presented a great technological challenge, and interesting schemes of reducing their effects have been forwarded. The most prominent of such noise sources will be discussed below.

4.1. *Laser noise*

The requirements on the quality ('purity') of the laser light used for the GW interferometry are a great technological challenge. As it happens, the light sources for the ground-based and the space-borne interferometers will both be Nd:YAG lasers, in the form of non-planar ring oscillators[20], see Figure 5. Pumped by laser diodes, they exhibit a high overall efficiency. Their good tunabilty allows efficient stabilization schemes.

Frequency stability A perfect Michelson interferometer (with exactly matching arms) would be insensitive to frequency fluctuations of the light used. The detectors will, however, by necessity have unequal arms, the ones on the ground due to civil engineering tolerances and a particular modulation scheme chosen, the space detector due to unavoidable imperfections in the orbits of the individual spacecraft.

Therefore, a very accurate control of the laser frequency is required, with (linear) spectral densities of the frequency fluctuations of the order $\widetilde{\delta\nu} = 10^{-4}\,\mathrm{Hz}/\sqrt{\mathrm{Hz}}$. Control schemes have been devised to reach such extreme stability, albeit only in the frequency band required, and not all the way down to DC (which would set an all-time record in frequency stability: $\widetilde{\delta\nu}\,/\,\nu = 3\times10^{-19}\,/\,\sqrt{\mathrm{Hz}}$).

Power stability Again due to asymmetries of the interferometer, the incoming laser beam needs to be closely controlled as to its power, in the frequency band

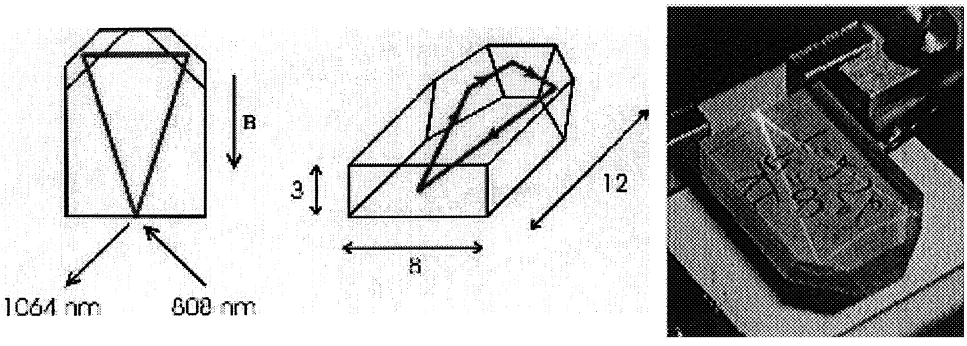

Fig. 5. NPRO laser, scheme, dimensions in mm (left), photo (right)

of interest. Here, however, a power stability in the order of 10^{-7} is seen to be sufficient[20].

Beam purity Any geometrical asymmetry of the Michelson interferometer will make it prone to noise from geometrical fluctuations of the laser beam. Thus the illumination of the Michelson is required to be an almost pure TEM_{00} mode. For small light powers, below 1 W as in the space project, this purity can be gotten by passing the light through a single-mode fiber. For the laser powers needed in the ground-based interferometers, however, a 'mode-cleaner' is used: a non-degenerate cavity that is tuned for the TEM_{00} mode, but suppresses the (time dependent) lateral modes that represent fluctuations in position, orientation, and width of the beam[21].

4.2. *Thermal noise*

All optical components – and in particular the mirrors – will cause fluctuations in the optical paths also due to their thermal vibrations, their *Brownian motion.* The noise coming from the pendulum modes of motion is most prominent at low frequencies, rolling off steeply towards higher frequencies. The noise due to the vibrational modes of the substrate rolls off less steeply and is thus a serious disturbance at intermediate frequencies.

By choice of materials (high mechanical Q) and appropriate shaping of the substrates (to keep their resonant frequencies above our kHz range) the effect of these thermal motions can be reduced.

Intensive research is going into the development and choice of appropriate materials for the mirror substrates (pure fused silica, sapphire), and the proper treatment for attaining the highest mechanical Q, e.g. several times 10^7. Such high values can be maintained only if the bonding to the suspension 'wires' does not introduce losses. Special bonding techniques are required using fibers of material identical to the substrate (monolithic suspension). Efficient collaboration between the European groups, under the leadership of the University of Glasgow, has given very promising results.

4.3. *Thermoelastic noise*

Only recently,[22,23] the effect of thermoelastic losses in the substrate material was recognized as another noise contribution. It scales with the thermal expansion coefficient squared and linearly with the thermal conductivity (which so far we always wanted to be high). This noise has thus become an important issue in the choice of appropriate materials, and it may even rule out the otherwise ideal sapphire.

4.4. *Seismic noise*

The mirrors between which the distances are to be monitored are suspended as pendulums in vacuum, to isolate them from extraneous vibrations: from seismic and acoustic noise.

Combinations of various schemes (pendulum suspension, lead-and-rubber stacks, even active position control) are used to reduce seismic noise by many powers of 10, which is relatively easy for frequencies above, say, 100 Hz. It is only with extreme effort that this lower frequency bound can be lowered to 10 Hz or less. Not only does the natural noise rise drastically towards low frequencies, but also the pendulum isolation becomes less effective. This causes the very steep rise to low frequencies in the righthand sensitivity curve in Figure 2.

VIRGO has developed an extremely powerful seimic isolation system, the "super-attenuator", consisting of a series of 6 successive pendulum stages, in conjunction with an 'inverted pendulum', and an active isolation stage. This suspension will allow VIRGO to extend GW search to lower frequencies than other terrestrial detectors. Figure 6 shows such an attenuator, with a total height of about 10 m. Preloaded cantilever springs in each stage provide excellent vertical isolation.

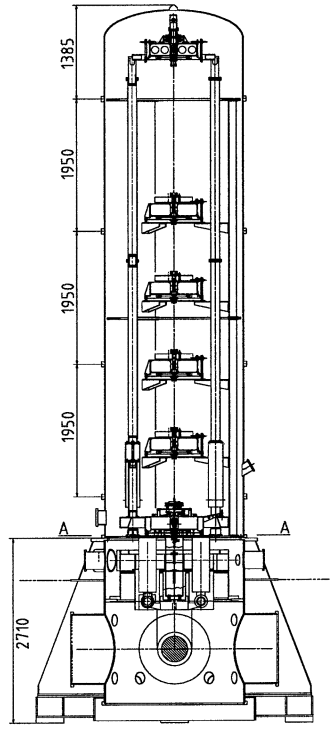

Fig. 6. Super-attenuator suspension in VIRGO

For both of the *thermal* noise effects, the internal vibrations of the mirrors as well as the pendulation mode, and also for the *seismic* disturbances, the sensitivity goal in strain of $h = 2\delta\ell/\ell$ can only be reached if we choose the armlength ℓ long enough. This is where our need for kilometer dimensions comes from. The steep rise at the left-hand side of the sensitivity curve "Earth" in Figure 2 is mainly due to the seismic and vibrational noise.

4.5. *Shot noise*

Particularly at higher frequencies, the sensitivity is limited by another fundamental source of noise, the so-called shot noise, a fluctuation in the measured interference coming from the "graininess" of the light. These statistical fluctuations fake apparent fluctuations in the optical path difference ΔL that are inversely proportional to the square root of the light power P used in the interferometer. The spectral density (in the 'linear' form we prefer) of the fluctuations of the path difference, $\widetilde{\Delta L}$, are described by

$$\widetilde{\Delta L} = \left(\frac{\hbar c}{2\pi}\frac{\lambda}{\eta P}\right)^{\frac{1}{2}} \tag{3}$$

where η is the conversion efficiency of the photo diode, and λ the laser's wavelength. For measuring the minute changes of the order of $\Delta L \sim 10^{-18}$ m in our kilometric "advanced" detectors, as much as 1 MW of light power, in the visible or the near infrared, would be required. This is not as unrealistic as it may sound; it can be realized by the concept of "power recycling".

4.5.1. *Power recycling*

The laser interferometers are planned to monitor the (gravitational-wave induced) changes δL of the light path by observing the dark fringe of the interferometer in one output port. The (unused) light going out at the other port of the beam splitter can be fed back, via a mirror M_P, and in correct phase with the incoming light (Figures 3, 4), so that the circulating light power is significantly enhanced. This scheme was proposed by Ron Drever in 1981, at the same time as Roland Schilling saw it come as a natural consequence in the Garching 30 m prototype, where the appropriate feedback had already been implemented for an efficient frequency stabilisation of the laser. The first implementations were done in that prototype: 1987 with only short arms, in 1996 with the full 30 m arm length[24].

To achieve the sensitivity goals of the current generation of gravitational wave detectors, the light power circulating in the interferometer needs to be of the order 10 kW. With lasers of 10 to 100 W and power recycling gains of 100 to 1000, such values are within current technology. The 1 MW possibly needed for the "advanced" detectors will, however, require some technological break-through, particularly in the preparation of sufficiently loss-free substrate materials.

4.5.2. *The shot noise limit*

Shot noise is a 'white' noise, but as the response in Eq. 2 rolls off as $1/f\tau$ at frequencies above the inverse storage time τ, the apparent strain noise rises proportional to frequency, as shown in the curves 'Space' and 'Earth' in Figure 2.

As we will see later, this frequency-proportional rise of the sensitivity curve will limit the space-borne interferometers in a similar way as here in the ground-based detectors.

4.6. *Advanced interferometry configurations*

An additional "recycling" scheme was later proposed by Brian Meers, and now forms the baseline for the GEO 600 interferometer: 'signal recycling' (SR) [14,15]. A further mirror, M_S, is added to the interferometer, this one in the output port (Figures 3, 4). The microscopic position of this mirror can be adjusted such that the signal sideband is also resonant in the interferometer, providing an enhancement of the signal, with possibly reduced measuring bandwidth. Schemes like this "signal recycling (SR)", or the related "resonant sideband extraction (RSE)" [16], are expected to be employed in future upgrades also of the other detectors. They can be used to optimize and tune the detector bandwidth independently of the carrier storage time in the arm cavities. Experimental verification of 'dual recycling', the combination of power and signal recycling, was given in 1995, albeit in a table-top setup [25].

The curve "*Earth*" in Figure 2 indicates the sensitivities that will eventually be reached with the current large interferometers, at least in their advanced versions.

4.7. *Next-generation ground-based detectors*

Even though the current detectors are not yet in full operation, it is essential to develop a next generation of detectors early on. The study of new technologies to be employed, of new materials, of advanced interferometric configurations has to be pushed forward, so that the necessary new implementations can be undertaken in or around the year 2005.

Three plans for such next-generation detectors have been put forward, which are entered in the lower part of Table 1: Advanced LIGO, LCGT, and EURO. The status of these three future projects will be sketched below.

Advanced LIGO Among these, the proposed US project is furthest progressed and well documented[26]. Advanced LIGO makes full use of the common efforts in the LIGO Scientific Collaboration, LSC. For locations, Advanced LIGO will rely on the existing facilities at the sites of Hanford and Livingston. The advantage is clear: no cost for new sites, for civil and vacuum engineering. One draw-back is that the incorporation of more "aggressive" approaches (cryogenics, all-refractive optics, Sagnac) is not so easy to realize, and that the option of lower seismic noise of underground sites is forfeited.

The Advanced LIGO groups of LSC have come up with simulations of the expected sensitivity that indicate that an operation limited only by the optics noise (shot noise, radiation pressure noise) appears possible. The suspension would have to be modeled after the GEO 600 triple pendulum concept, mirrors be made from large substrates of sapphire (or YAG), and the schemes of SR or RSE, developed at GEO, have to be used.

As was recently shown by Buonanno and Chen[29], the 'detuned' implementation of SR/RSE can even lead to a (moderate) reduction of what is usually termed the 'Standard Quantum Limit'.

LCGT The concept of the Japanese project "Large Cryogenic Gravitational-Wave Telescope" (LCGT) is also rather well defined;[27] it will use super-cooled (cryogenic) mirrors. The location of LCGT will be deep inside the mountain that houses the famous neutrino detector Super-Kamiokande. The ground noise is by nearly two orders of magnitude lower than at ground level. The armlength will be 3 km, and an existing tunnel can be used for one arm. Funding is not yet secured.

EURO Even more ambitious is the concept of the European detector EURO[28]. The four funding agencies (CNRS, MPG, INFN, PPARC) of France, Germany, Italy, and the UK, agreed to pursue the definition of a common European high-sensitivity detector. However, the completion and the commissioning of the current projects, GEO 600 and VIRGO, has the highest priority. Thus, the actual beginning of the project may be as late as 2008. A site deep underground (as for LCGT) is preferred, but not yet decided upon.

Simulations using parameter sets from optimistic but not unreasonable assumptions, verified that an operation limited only by the (quantum-)optical noise, i.e. solely by shot noise and radiation pressure noise, seems possible, using classical techniques, but going to the ultimate frontier of current technologies.

4.8. *The technological challenge in advanced detectors*

The technology required in the proposed future detectors is at the forefront of current technology, and even beyond. Many new developments are being pushed just by this goal of improved gravitational wave detectors, but it is fortunate that some other developments required are also driven by commercial interest.

Optical materials Of great importance is the effort to develop better optical materials. The high light powers (up to the order of Megawatt!) will require extremely low absorption losses, in the reflective and anti-reflective coatings in reflection, as well as in the bulk material of the substrate in transmission. Three materials have the greatest promise: (1) very pure fused silica, specially prepared to have low OH-content, for low absorption, (2) sapphire single crystals, having a naturally low absorption, but with a high constant of birefringence, (3) YAG (Yttrium aluminum garnet) as used for laser crystals.

For all three materials, the great technological challenge is to produce substrates of the order of half a meter in diameter, and of similar thickness, with a high level of homogeneity. For substrates of the end mirrors, which do not require light transmission, also silicon is a possible option. Proposals are also being made to use all-diffractive optics to avoid the problems of light transmission altogether.

High mechanical Q At the same time, to keep thermal vibrations low, the optical components need to have extremely high mechanical quality Q. Investigation into the properties of the materials (see above) are carried out by several institutions, and values of the order $Q \sim 10^7$ at room temperature and 10^9 at cryogenic temperatures have been accomplished [30,31]. And also much research was done on how to suspend these components in such a way as to preserve their high Q [30,31].

5. The space interferometer LISA

Only a space mission allows us to investgate the gravitational wave spectrum at very low frequencies. For all ground-based measurements, there is a natural, insurmountable boundary towards lower frequencies. This is given by the (unshieldable) effects due to varying gravity gradients of terrestrial origin: moving objects, meteorological phenomena, as well as motions inside the Earth. To overcome this "brick wall", the only choice is to go far enough away, either into a wide orbit around the Earth, or better yet further out into interplanetary space. Once we have left our planet behind and find ourselves in outer space, we have some great benefits for free: to get rid of terrestrial seismic and gravity gradient noise, to have excellent vacuum along the arms, and in particular to be able to choose the arm length large enough to match the frequency of the astrophysical sources we want to observe.

5.1. *The LISA configuration*

The European Space Agency, ESA, and NASA have agreed to collaborate on such a space mission called LISA, "Laser Interferometer Space Antenna"[32,33].

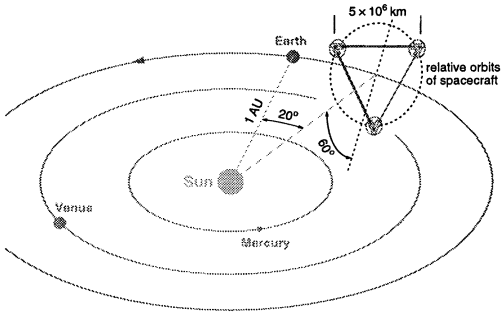

Fig. 7. Orbits of the three spacecraft of LISA, trailing the Earth by 20°. The triangle arms are scaled by factor 10.

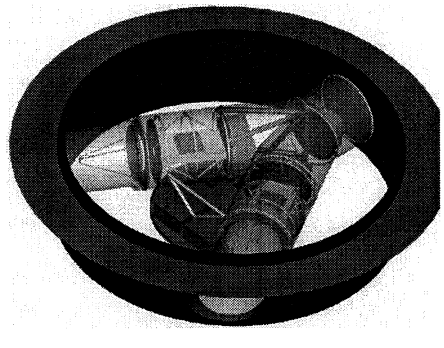

Fig. 8. View of one LISA spacecraft, housing two optical assemblies. The solar panel at top not shown, the thermal shield shown as semi-transparent.

LISA consists of three identical spacecraft, placed at the corners of an equilateral triangle (Figure 7). The sides are to be 5 million km long (5×10^9 m). This triangular constellation is to revolve around the Sun in an Earth-like orbit, about 20° (i.e. roughly 50 million km) behind the Earth. The plane of this equilateral triangle needs to have an inclination of 60° with respect to the ecliptic to make the common rotation of the triangle most uniform. The small orbit correction manoeuvres required can be made with field-effect ion thrusters. The three spacecraft form a total of three, but not independent, Michelson-type interferometers, here of course with 60° between the arms.

The spacecraft at each corner will have two optical assemblies that are pointed, subtending an angle of 60°, to the two other spacecraft (indicated in Figure 8, with

the Y-shaped thermal shields shown semi-transparent). An optical bench, with the test-mass housing in its center, can be seen in the middle of each of the two arms, and a telescope of 30 cm diameter at the outer ends. Each of the spacecraft has two separate lasers that are phase-locked so as to represent the "beam-splitter" of a Michelson interferometer.

5.2. *Annual orbit of LISA*

During its yearly motion around the sun, the three spacecraft of LISA will 'roll' on a cone of half-angle 60°, as indicated in Figure 9. Each spacecraft moves on a slightly elliptic orbit around the sun, as indicated for one spacecraft by the lighter orbit, slightly tilted with respect to the (heavier) Earth orbit.

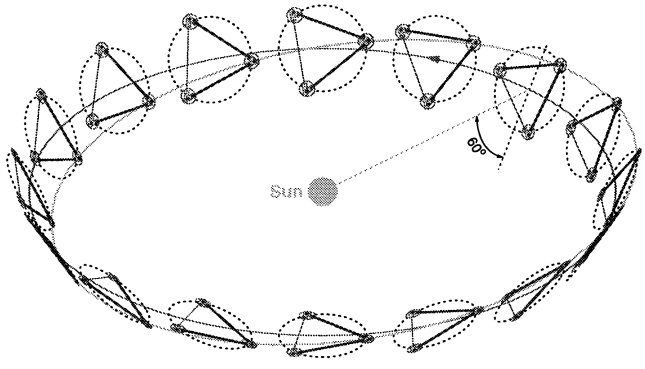

Fig. 9. Annual motion of the LISA configuration: the heavier orbit represents the Earth's orbit, and the orbit on which the center of the LISA triangle circles the sun. The motion of one of the LISA spacecraft is indicated by the (slightly inclined) lighter orbit.

This configuration has a number of advantages that make several of the design requirements less stringent.

Constant angle to Sun The spacecraft face the sun by a constant angle of incidence of 30°, which provides a very stable thermal environment for the sensitive parts (optical assembly, the sensors) of the spacecraft. It also allows a design of the spacecraft such that no sunlight will ever enter the sensitive optical assembly.

Constant triangle shape The rather unperturbed orbits of the three spacecraft provide a very stable configuration, very close to an equilateral triangle. The maximum changes in the ($\approx 60°$) angles subtended by the lines of sight to the other two spacecraft are in the order of 1°. Thus it is relatively easy to devise articulation schemes for the two 'telescopes' in each spacecraft to follow these small angle deviations. The maximum distance variations are in the order of 100 000 km, which is also small when compared with the very large baseline of 5 million km: $\approx 2\,\%$.

Constant distance to Earth The center of the LISA triangle trails the Earth in its orbit by 20°, or about 50 million km. This makes the distance to

Earth, for radio communication, also quite stable, which reduces the problems of radio antenna design and radio transmission power.

The radio antennas must, however, provide a rotational degree of freedom that allows them to be pointed towards the Earth for the (intermittent) data transmissions, as well as for the (probably continuous) preparedness for control signals from Earth.

5.3. *Gravitational sensors*

The distances between the different spacecraft are measured from test masses housed *drag-free* in these three spacecraft. The three LISA spacecraft each contain two test masses, one for each arm forming the link to another LISA spacecraft. The test masses, 4 cm cubes made of an Au/Pt alloy of low magnetic susceptibility, reflect the light coming from the YAG laser and define the reference mirror of the interferometer arm. These test masses are to be freely floating in space.

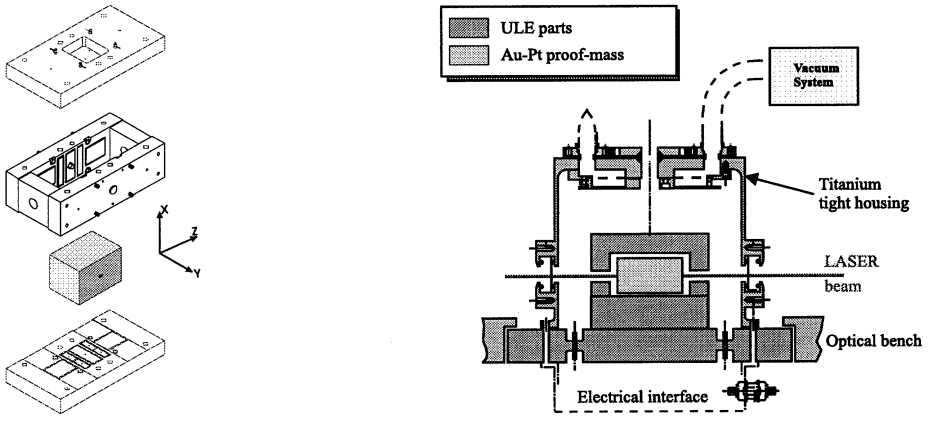

(a) The sensor cage (b) Sensor configuration

Fig. 10. Layout of gravitational sensor: (a) exploded view, (b) with housing.

For this purpose these test masses are also used as inertial references for the drag-free control of the spacecraft that constitutes a shield to external forces. Development of these sensors is done at various institutions. Figure 10 shows a sensor modelled after already space-proven developments at ONERA[34], other configurations are being discussed[35].

These sensors feature a three-axis electrostatic suspension of the test mass with capacitive position and attitude sensing. A resolution of $10^{-9}\,\mathrm{m}/\sqrt{\mathrm{Hz}}$ is needed to limit the disturbances induced by relative motions of the spacecraft with respect to the test mass: for instance the disturbances due to the spacecraft self-gravity or to the test-mass charge.

5.4. *FEEP thrusters*

The very weak forces required to keep up drag-free operation, less than 100 μN, are to be supplied by field-effect electrical propulsion (FEEP) devices: a strong electrical field forms the surface of liquid metal (Cs or In) into a cusp from which ions are accelerated to propagate into space with a velocity (of the order 60 km/s) depending on the applied voltage. Such FEEP thrusters have been developed at various European institutions, namely Centrospazio, Italy[36] and Seibersdorf, Austria[37], their characteristics will be studied in a technology demonstration mission (Section 5.7).

5.5. *Noise in LISA*

This section will cover some of the most worrying noise sources in the LISA project, which then will also be relevant for the project ASTROD.

Figure 2 showed sensitivity curves for the ground-based interferfometers, as well as for LISA. In both cases the shape is that of a trough, with a steeper slope at the left than on the right. The curve for LISA is again shown in Figure 11, enlarged and in greater detail. That LISA sensitivity curve consists of three main parts, as indicated by the three differently shaded frequency regions, in which different noise mechanisms take hold.

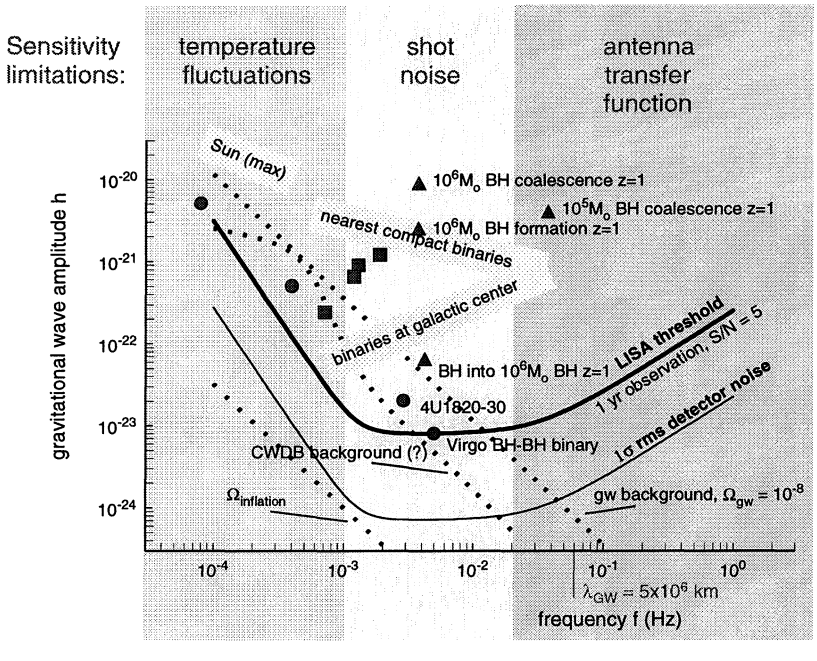

Fig. 11. Sensitivity of LISA: the heavy curve "LISA threshold" represents the signal strength that would provide a signal-to-noise ratio of 5 if averaged over one year, and over all possible directions and polarization angles. Major noise contributions are indicated by different shading.

5.5.1. *Shot noise*

With the 30 cm optics planned, from 1 W of infrared laser power transmitted, only some 10^{-10} W will be received after 5 million km, and it would be hopeless to have that light reflected back to the central spacecraft. Instead, also the distant spacecraft are equipped with lasers of their own, phase-locked to the incoming laser beam.

Due to the low level of light power received, shot noise plays a major role in the total noise budget of spurious displacements. It is responsible for the flat middle part of the sensitivity curve.

The effect of shot noise is a spurious 'path difference' $\widetilde{\delta L}$ inversely proportional to the power P available for interferometry, in the case of LISA, at arm lengths of 5 million km, this received power is of the order 10^{-10} W. With an increased armlength, perhaps to the order of 2 AU, i.e. 300 million km, the power would decrease by a factor of 60^2, and both the apparent spurious path differences $\widetilde{\delta L}$ and the optical path L would thus increase by an identical factor of 60. This means that the sensitivity of a space probe, other characteristics remaining the same, would have a shot noise limit for the strain $h \sim \delta L/L$ that is independent of the armlength, $L/2$. This fact will be of importance in the estimates of ASTROD's sensitivity.

5.5.2. *Antenna transfer function*

Again, as shown in Section 4.5.2, we have to consider that the antenna response rolls off as $1/f\tau$ at frequencies f above the inverse of the round-trip time τ. Thus at these frequencies the shot noise leads to the frequency-proportional rise at the right-hand side of the sensitivity curve in Figure 2 and, in more detail, in Figure 11.

5.5.3. *Acceleration noise*

At frequencies below 1 mHz, the noise is mainly due to accelerations of the test mass that cannot be shielded even by the drag-free scheme: forces due to gravitating masses on the spacecraft when temperature changes their distances, charging of the test masses due to cosmic radiation, residual gas in the test mass housing. Except for the cosmic ray charging, the acceleration noise contributions are dependent on temperature variations, and this is why in Figure 11 they come under the heading 'temperature fluctuations'.

These accelerations have a rather 'white' spectral distribution, which thus results in position errors rolling off roughly as $1/f^2$.

Gravity gradient noise The test mass, housed in the LISA spacecraft, is subject to the gravity field of the other masses that form part of the spacecraft. These masses, though 'rigidly' connected to each other, will undergo small changes in their positions, due, e.g., to the changes in temperature distribution.

This thermal distortion of the spacecraft actually is one of the most prominent sources of 'acceleration noise'. Elaborate calculations on the temperature fluctua-

tions to be expected (e.g. from variations in the solar radiation) and on the thermal behavior of the spacecraft's masses have resulted in a set of requirements for the LISA design[33].

Noise due to charging of the test mass Cosmic radiation will cause the test mass to acquire an electrical charge, which will result in a number of noise effects. A broad discussion is given in the LISA Pre-Phase A Study (PPA2)[32].

These charges will give rise to electrostatic forces of attraction to the cage walls. The charges will also, if not perfectly shielded by the cage and the spacecraft shields, be subject to Lorentz forces due to LISA's motion in the interplanetary magnetic field. And, similarly, changes in that magnetic field will also produce forces on the test mass.

As remedies, the test mass will be quite well shielded from outside fields, and in particular, the charge that has accumulated on the test mass will be monitored, and from time to time a discharge by shining ultraviolet light on the test mass, will be carried out[32].

Noise due to residual gas A very wide field of acceleration noise contributions is due to the residual gas inside the sensor. Although the vacuum will have high quality, 10^{-8} mbar $= 10^{-6}$ Pa, the test mass will be subject to several non-negligible accelerations.

Foremost among these can be the stochastic noise due to the buffeting by the impinging residual gas molecules. This statistical noise is proportional to the square root of the residual gas pressure, p.

If the casing of the sensor has a temperature gradient, due, e.g., to changes in solar radiation or in the power dissipation in the spacecraft electronics, differences in gas pressure inside the sensor will build up. Here we must mention the so-called radiometer effect, but perhaps even more worrisome the effect of temperature-dependent outgassing of the cage walls.

5.5.4. *Noise total*

With a myriad of other, smaller, noise contributions the total apparent path noise amounts to something like $\widetilde{\delta L} \approx 40 \times 10^{-12}\,\mathrm{m}/\sqrt{\mathrm{Hz}}$ at the lowest part, the bottom of the trough. For signals monitored over a considerable fraction of a year, the best sensitivity is about $h \approx 3 \times 10^{-24}$, indicated in Figure 2 by the curve marked "Space", and in more detail in Figure 11.

5.5.5. *The LISA prospects*

Some of the gravitational wave signals are guaranteed to be much larger. Failure to observe them would cast severe doubts on our present understanding of the laws that govern the universe. Successful observation, on the other hand, would give new insight into the origin and development of galaxies, existence and nature of dark matter, and other issues of fundamental physics.

5.6. *Status of LISA*

LISA is approved by ESA as a cornerstone mission under Horizons 2000. A System and Technology Study[33] has substantiated that improved technology, lightweighting, and collaboration with NASA will lead to a considerable reduction of cost. Thus, a new, *faster, cheaper, and better* approach, together with NASA, is being pursued, under the auspices of an international LISA Science Team. Launch is foreseen for 2011, not very long after first operation of the next-generation ground based detectors. LISA has a nominal lifetime of 2 years, but the equipment and thruster supply are chosen to allow even 10 years of operation.

A collection of papers given at the *Third International LISA Symposium, 2000,* is presented in a special issue of Classical and Quantum Gravity[38].

5.7. *Technology demonstrator*

Some of LISA's essential technologies (gravitational sensor, interferometry, micronewton thrusters) are to be tested in a mission LTP (LISA Technology Package) on board an ESA SMART-2 satellite.

The package will contain, on a common optical bench, two gravitational sensors, similar to the one of Section 5.3. The relative motion between the two freely floating test masses will be monitored with high accuracy by interferometry. The sensitivity in this (scaled-down) experiment will come to within one power of ten to the proposed LISA sensitivity.

This package is to be flown in a geocentric orbit relatively far away from Earth, so as to avoid the many disturbances near the Earth. The same mission SMART-2 might also host the NASA probe ST-7. Launch is definitely set for August 2006.

5.8. *LISA follow-on*

Even as early as now concepts are being discussed for a successor to LISA, on the possible enhancements in sensitivity and/or frequency band. One scheme would try to bridge the frequency gap between ground and space detectors, by reducing the arm lengths, leaving the general configuration unchanged. Another concept is to have a square constellation instead of the triangle, providing pairs of independent interferometers. These can be used to detect and measure a stochastic background of gravitational waves, similar to, but reaching much further back than the 3 K electromagnetic background radiation.

ASTROD will extend to a low-frequency range not fully covered by LISA, and thus it would be – given similar sensitivity – a further useful extension in the search for and measurement of gravitational waves.

6. Proposed space project ASTROD

This "School and Symposium" is dedicated to the space project ASTROD,[39] a mission with three spacecraft, all three in solar orbits similar to the Earth's orbit.

Figure 12 gives a notion of the orbits of the three spacecraft. While the main targets of ASTROD will be the measurement of relativistic effects in the solar environment, a possible additional application might be the measurement of gravitational waves. It is only this latter objective that will be discussed in this paper.

Due to the different orbit parameters, after starting from identical positions, the three spacecraft will drift away from each other, and at times will have constellations resembling the equilateral triangle of LISA, only by a factor 50 or so bigger. This larger armlength will make ASTROD particularly useful at extremely low frequencies.

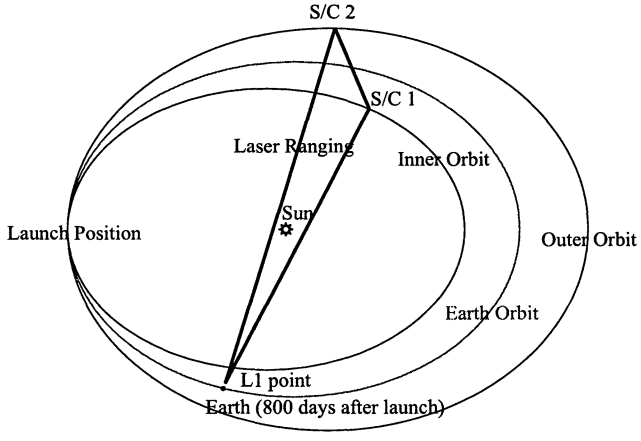

Fig. 12. Orbits of the three ASTROD spacecraft, SC 3 near Earth

The detection principle in ASTROD will be modelled after that of LISA: test masses in sensors will be the references for the interferometric measurement of changes in distance. In the design of these sensors, the ASTROD project will be able to draw from the experience gained in the 'LISA Technology Package' LTP (to fly in 2006) and then later in LISA itself (2011).

6.1. *ASTROD sensitivity*

So far, no dedicated study of the ASTROD sensitivity has been made. Rather, the plot to be presented here, as well as the ones published in the special volume on ASTROD[40], are based on extrapolations from the LISA sensitivity curves. Such an extrapolation, based on current LISA technology, is presented in Figure 13.

In the sensitivity as measured in strain $h \sim \Delta L/L$, the longer arm length of ASTROD is favorable, as one divides by an optical path L that is by a factor 30 to 60 larger. But this rule has to be treated separately for the three noise regimes correcponding to the three shaded areas in the LISA sensitivity plot of Figure 11.

The flat region The white-noise part, where the sensitivity is practically frequency-independent, would remain at the same strain level, as the higher value of the arm length L is compensated by the loss in light power by the square of that

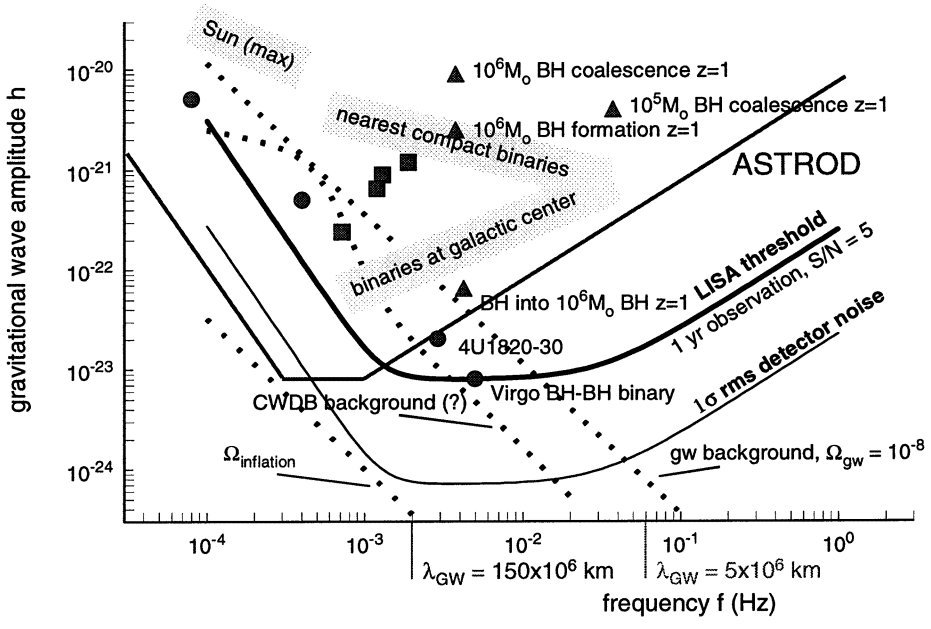

Fig. 13. Sensitivity of ASTROD: the straight solid lines "ASTROD" are inserted in the LISA sensitivity drawing of Figure 11. Again the sensitivity is that of averaging over all angles of incidence and polarization, and over one year of observation time.

length, which then gives rise to a shot-noise level rising linearly with length L. This fact had already been pointed out in Section 5.5.1.

The antenna response region The rise on the right-hand side also results from the (white) shot noise, but taking into account the reduced response to actual GW signals. This response rolls off roughly as Λ_{GW}/L, once the optical path L exceeds $\Lambda_{GW}/2$. Thus the rise in the noise curve sets in at lower frequencies for longer arms, and this can be expressed as a shift in frequency to the left that goes linearly with the increase in arm length L.

The acceration noise region The longer arm length will also reduce all acceleration-induced noises (at the low frequency side) by just this factor of length increase. So it can be extrapolated from the LISA curve by an appropriate, length-proportional shift downwards, i.e. to lower noise levels. That left-hand part has a slope roughly proportional to $1/f^2$, and so we can also re-draw that slope by shifting it horizontally (i.e., in *frequency*) by only the *square root* of the length factor.

The ASTROD noise curve So in actual fact, the flat part will become narrower as the arm length L increases, and there would be an arm length when that flat part is eaten up by the linear shift to the left of the right-hand slope and the smaller square-root shift of the left-hand slope.

This estimate, based on LISA technology of today, would lead to a sensitivity as sketched roughly by the three straight lines "ASTROD" in Figure 13.

It is to be hoped that by the time of building ASTROD, some further progress in the noise reduction in the sensors can be made, and that the limiting left-hand line can then be pushed further to the left, i.e. to lower frequencies, as shown, e.g., in W.-T. Ni's contribution[39]. To achieve this, however, would require a reduction by that same factor of arm-length gain, e.g., 50.

6.2. *Challenges in ASTROD*

Even though in some respects ASTROD will be modelled after LISA, there will be various details where the technological requirements are much more challenging. None of these obstacles will be insurmountable, but they will require a painstaking investigation and much experimental verification.

Low-power interferometry Whereas LISA had powers available in the order of 10^{-10} W, ASTROD will have only 3×10^{-14} W. To do interferometry with such low powers, and to phase-lock the local lasers to that low incoming power, will be an important issue. Progress in the 'art' of low-power detection is being made (see Liao et al.[41]), and again the LISA project will point the way, but the ASTROD situation is by orders of magnitude more challenging.

Inclination to sun It is a fortunate feature that the LISA spacecraft will through their entire lifetime have a constant inclination to the sun of 60° (see Figure 9). This leads to very stable thermal conditions inside the spacecraft. The ASTROD spacecraft will not have such a favorable constant inclination. More elaborate thermal shielding inside the spacecraft will be required to maintain a similarly benign environment for the sensor.

Direct sun light The LISA inclination will guarantee that never will direct light from the sun enter the very sensitive optical detector. For ASTROD, on the other hand, the measurements of possible relativistic effects requires light paths that pass very close to the sun. Only with elaborate coronograph systems will these measurements be possible. The measurement of gravitational waves will, however, be made at times when the ASTROD constellation does not have paths close to the sun, so then the problem does not arise.

7. LISA data analysis

Due to the low frequency band of the LISA detection, the data rate is rather low, and thus the total amount of data. Data will be collected on-board, and transmitted to Earth once per two to three days.

The very limited transfer rate from spacecraft to Earth would not allow much more than the envisaged 1.5 kbit/sec. But such a low data rate is possible only due to a great load of data analysis and data reduction being done on-board. That is particularly true if the schemes of 'time-delay interferometry' are to be utilized (see Section 8).

7.1. *Directivity*

LISA, as all interferometric GW detectors, has a preferred direction and a preferred polarization of the incoming gravitational wave. This would cause an antenna, fixed in space, to be particularly sensitive in some directions, and totally blind in others.

The annual motion of LISA will, however average out these types of directivity, as LISA is facing different locations at the sky, and with different preferred polarization directions at different times, see Figure 9 in Section 5.2. This is why the sensitivity curves in Figures 11 and 13 for a signal-to-noise ratio of 5 is drawn by factor of $5\sqrt{5} = 11.2$ higher than the lower curve.

On the other hand, LISA's detection can make use of the 'signature' that continuous-wave signals will have, due to the changing response sensitivity, and due to the Doppler shifts that the signal will undergo as LISA approaches and recedes from the source during its annual orbit.

A detailed analysis of the LISA sensitivity under these assumptions was made by R. Schilling[42,32]. One important result was that the drastic drops in sensitivity for gravitational waves with wavelengths fitting into the armlengths are benignly smoothed out in this averaging, as will be seen in the curve of Figure 15.

7.2. *Noise due to fluctuating laser frequency*

The strength of the Michelson-interferometer scheme is that the high symmetry between the two arms makes the interferometer insensitive to a number of fluctuations of the illuminating light source. The most serious of these is the fluctuation in laser phase, $\delta\phi$, or in frequency, $\delta\nu$. Any change in laser frequency will cause spurious signals proportional to the difference in arm lengths.

In the simplest case of a Michelson interferometer, the phases ϕ_i accumulated in the round-trips in the two arms are measured, $s_i(t) = \phi_i(t) - \phi_i(t - 2T_i)$, and then compared with each other:

$$\Phi(t) = s_1(t) - s_2(t) = \phi_1(t) - \phi_1(t - 2T_1) - \phi_2(t) + \phi_2(t - 2T_2)\,. \tag{4}$$

In each arm, the current laser phase is compared with the (echoed) phase of one round trip ago, these times $2T_1$ and $2T_2$ differing by a relatively small misalignment $\Delta = 2T_1 - 2T_2$. For the sake of simplicity let us also assume equal laser phase $\phi_1(t) = \phi_2(t) = \phi_0 + \delta\phi(t)$ in the two arms, with a phase noise component $\delta\phi(t)$. Clearly, for unequal round-trip times T_i, the error $\delta\Phi(t)$ would become

$$\delta\Phi(t) = \frac{\mathrm{d}}{\mathrm{d}t}\,\phi(t - 2T)\,(2T_1 - 2T_2) = 2\pi\delta\nu(t - 2T)\,\Delta\,. \tag{5}$$

The celestial mechanics of the LISA orbits will cause relative armlength variations in the order of 10^{-2}, and these would produce spurious signals from the natural laser frequency fluctuations well above the true gravitational wave signals.

8. Unequal armlength interferometry

Even if the laser frequency is well stabilized to the best of current technology, perhaps to $30\,\mathrm{Hz}/\sqrt{\mathrm{Hz}}$, a drastic further reduction of the effect is required. Here, a scheme first proposed by Giampieri et al.[43], and then optimized with respect to the suppression of several LISA error sources[44,45,46], promises a significant improvement. The concept of Giampieri et al. was to estimate, from the phases measured separately for each arm and each spacecraft, the underlying laser phase noise and appropriately correct for it. This scheme operates in the frequency domain.

The approach to be discussed below, operating in the time domain, will offer even better compensation of the laser noise, and it is the current baseline for LISA [33].

8.1. *Time delay interferometry*

The basic principle of the method is best demonstrated using the simplified case of a Michelson interferometer with only one master laser, and the phase measurements done in only one spacecraft. What is used is a linear combination of the read-out data s_i with data additionally delayed, in each arm by the travel time in the other:

$$X(t) = s_1(t) - s_2(t) - s_1(t - 2\tau_2) + s_2(t - 2\tau_1)\,, \tag{6}$$

where the delays τ_i are chosen to equal the true travel times T_i. It is easily verified that this algorithm can fully cancel the laser phase noise $\delta\phi(t)$.

One can estimate what degree of cancellation could be achieved if there were slight deviations $\delta_i = 2T_i - 2\tau_i$ between the true round-trip times T_i and the delay times τ_i used in Eq. (6).

The laser phase noise in the measurements taken in the two arms will have the general form $\delta s_i(t) = \delta\phi(t) - \delta\phi(t - 2T_i)$, so that Eq (6) will lead to a total phase error of

$$\begin{aligned}\delta\Phi(t) = {} & \delta\phi(t) - \delta\phi(t - 2T_1) - \delta\phi(t - 2\tau_2) + \delta\phi(t - 2T_1 - 2\tau_2) \\ & - \delta\phi(t) + \delta\phi(t - 2T_2) + \delta\phi(t - 2\tau_1) - \delta\phi(t - 2T_2 - 2\tau_1)\,.\end{aligned} \tag{7}$$

The undelayed terms $\delta\phi(t)$ cancel right away. And clearly, for $\tau_i = T_i$, this combination of noise terms cancels fully, regardless of any difference in the values for T_1, T_2. If, however, we have small deviations of the assumed values τ_i from the true round-trip times T_i, we must evaluate Eq. (7) for plausible values of T_i, τ_i.

8.2. *The LISA case of almost equal arms*

The typical LISA case would be a relatively small difference Δ between the two round-trip times, $\Delta = 2T_1 - 2T_2$, and also we will assume the delay time errors $\delta_i = 2\tau_i - 2T_i$ to be relatively small. Then we can consider appropriate difference terms in Eq. (7) as derivatives at a mean time $t - 2T$:

$$\begin{aligned}-\delta\phi(t - 2T_1) + \delta\phi(t - 2T_2) &\approx \delta\omega(t - 2T) \cdot (\Delta) \\ +\delta\phi(t - 2\tau_1) - \delta\phi(t - 2\tau_2) &\approx \delta\omega(t - 2T) \cdot (-\Delta - \delta_1 + \delta_2)\,.\end{aligned} \tag{8}$$

Thus, the terms with delays of $2T$ and $4T$ result in phase errors of

$$\begin{aligned}\delta\Phi(t)\big|_{2T} &\approx \delta\omega(t-2T)\cdot(-\delta_1+\delta_2)\\ \delta\Phi(t)\big|_{4T} &\approx \delta\omega(t-4T)\cdot(\delta_1-\delta_2)\,.\end{aligned} \tag{9}$$

In this approximation, the errors δ_1, δ_2 in guessing the round-trip times T_1, T_2 would still not result in an error $\delta\Phi$ if they happened to be identical: $\delta_1 = \delta_2$, and they would be disturbing the most if they had opposite sign.

Furthermore, at very low frequencies, the laser frequency noise $\delta\omega$ would not change drastically from delay $2T$ to $4T$. So then the terms of delays $2T$ and $4T$ would cancel to a large extent, regardless of the error difference $\delta_1 - \delta_2$. This is, however, very similar to the reduction in response to the genuine GW signals and will thus lead to neither an improvement nor a deterioration of the noise introduced by the mis-estimates $\delta_1 - \delta_2$. For noise frequencies f at which the argument $2\pi f\,\Delta$ becomes significant (say, ≈ 1), this low-frequency cancellation ceases.

With the allowance in optical-path noise for the laser phase noise of $\widetilde{\delta\mathcal{L}} = 10\times10^{-12}\,\mathrm{m}/\sqrt{\mathrm{Hz}}$ (total, from four spacecraft, see PPA2[32]), and with the LISA laser stability of $\widetilde{\delta\nu} < 100\,\mathrm{Hz}/\sqrt{\mathrm{Hz}}$, the allowable delay-time error $\delta_1 - \delta_2$ would be

$$|\delta_1-\delta_2| < \frac{\widetilde{\delta\mathcal{L}}}{c}\Big/\frac{\widetilde{\delta\nu}}{\nu} = 10^{-11}\,\frac{\mathrm{m}}{\sqrt{\mathrm{Hz}}}\Big/\left(100\,\frac{\mathrm{Hz}}{\sqrt{\mathrm{Hz}}}\times10^{-6}\,\mathrm{m}\right)\approx 10^{-7}\,\mathrm{s} \tag{10}$$

corresponding to 30 m. A more detailed analysis is given in Tinto et al.[46].

8.3. *The case of grossly unequal arms*

When the round-trip times T_1 and T_2 are no longer rather similar, as will be the case for ASTROD, the delay time errors δ_1 and δ_2 will enter with different factors, as becomes evident from Eq. (7). The application of the same idea as before will lead to the error of the once-delayed terms

$$\delta\Phi(t)\big|_{2T} \approx -\delta\omega(t-2T_1)\,\delta_1 + \delta\omega(t-2T_2)\,\delta_2\,, \tag{11}$$

now with very different T_1, T_2. For the twice-delayed terms, on the other hand, the factors are identical (in absolute value), and we have

$$\delta\Phi(t)\big|_{2T_1+2T_2} \approx \delta\omega(t-2T_1-2T_2)\cdot(\delta_1-\delta_2)\,. \tag{12}$$

There is no longer a combination (the "common mode" error $\delta_1 = \delta_2$) that will nullify the errors $\delta\Phi(t)\big|_{2T}$ and $\delta\Phi(t)\big|_{2T_1+2T_2}$ simultaneously.

Configurations with intentional strong armlength differences have recently been analyzed[47]. With ASTROD's armlengths strongly varying with time, a near-equal armlength configuration will hardly ever exist. Therefore it will be important to investigate, with feasible assumptions on the laser phase noise, the armlengths, and the required sensitivity, down to what accuracy the τ_i need to be known.

8.4. *The LISA analysis algorithms*

How powerfully the *time delay interferometry* cancels out not only laser phase noise, but also other instrumental errors is shown in various papers by Armstrong, Estabrook, and Tinto [44,45,46]. These form the baseline for the LISA procedure[33]. It is assumed that phase measurements are made in all three spacecraft, each equipped with independent lasers, with independent highly stable clocks (USOs), and with an intraspacecraft link between the two lasers on board each spacecraft.

Figure 14 shows four types of such configurations. The nominal LISA configuration is an unequal-arm Michelson interferometer, as in Figure 14, top left. The

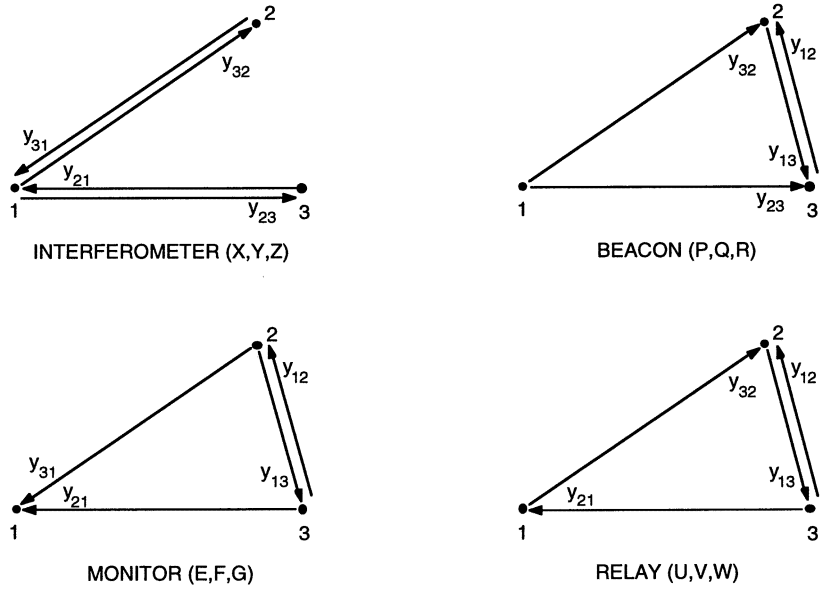

Fig. 14. The four types of four-link LISA data combining possibilities.

links from one spacecraft to another are specified by two indices, of which the first one indicates the arm (via the number of the spacecraft opposite that arm), and the second one the direction (via the target spacecraft). Indices after a comma will indicate the individual delays of the data, again by specifying the arm via the opposite spacecraft. Multiple (up to fourfold) delays are used. One typical example (the Michelson configuration of Figure 14, upper left) would look like this:

$$\begin{aligned} X = {} & y_{32,322} - y_{23,233} + y_{31,22} - y_{21,33} + y_{23,2} - y_{32,3} + y_{21} - y_{31} \\ & + \frac{1}{2}\left(-z_{21,2233} + z_{21,33} + z_{21,22} - z_{21}\right) \\ & + \frac{1}{2}\left(+z_{31,2233} - z_{31,33} - z_{31,22} + z_{31}\right) \end{aligned} \tag{13}$$

This set of time-domain combinations of the y_{ij} from the two arms and from the intraspacecraft signals z_{ij} cancels all noise due to laser phase fluctuations and to motions of the optical benches[44,45]. In a different approach,[46] the frequency fluctuations of lasers and USOs can all be cancelled.

It is assumed that shot noise and optical path noise (i.e. total optical path noise, as specified in PPA2[32]) have the same transfer functions. The LISA sensitivity would then have the form given in Figure 15, again averaged over one year, and over all directions of propagation and polarization, and for SNR = 5. This is where the shape of the (simplified) sensitivity curves of Figures 11 and 13 comes from.

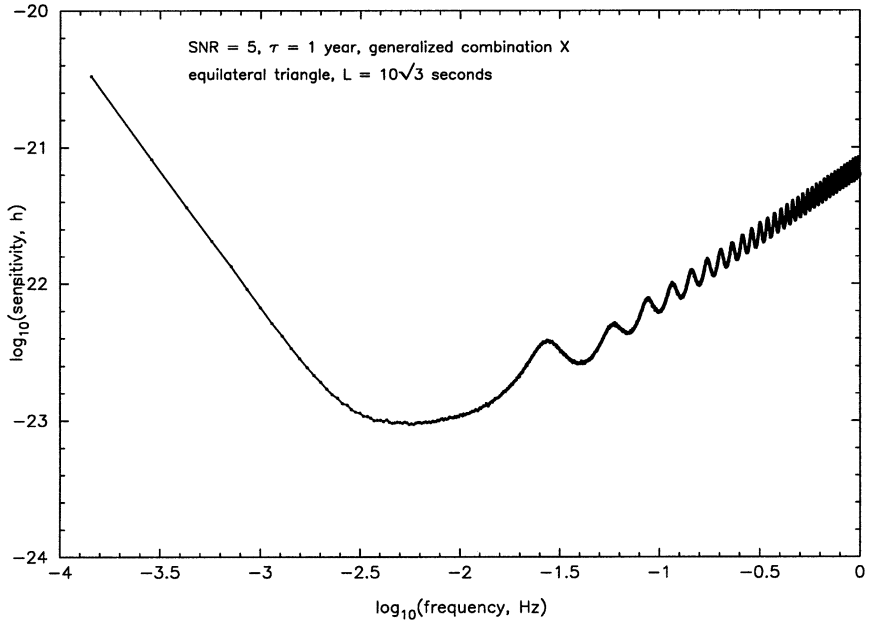

Fig. 15. Sensitivity plot for the unequal arm combination of Figure 14, top left (Michelson)

8.5. *Constancy of arm lengths*

A sufficient equality of the (three) armlengths cannot be maintained by LISA, the arms of which will have annual changes in length of the order 100 000 km. The variation in ASTROD will be even larger, by orders of magnitude. Thus the above data analysis needs to be employed to suppress faked signals resulting from short-term fluctuations in laser frequency. These schemes require a *knowledge* of the lengths of the arms to better than 30 m to be able to apply the proper time delays to the various time series.

The processing techniques[45,46] required for LISA to cancel out fluctuations in laser frequency and position of the test mass inside the sensor will also have to be

applied in the case of ASTROD. In LISA, the application is relatively easy, as the arm lengths are rather well constant throughout the course of the year. For ASTROD, the arm lengths change much more rapidly, and by much larger amounts. So an increased effort has to be made to render the LISA data-analysis routines applicable also under these more challenging conditions.

9. Conclusion

The difficulties (and thus the great challenges) of gravitational wave detection stem from the fact that gravitational waves have so little interaction with matter (and space), and thus also with the measuring apparatus. Great scientific and technological efforts, large detectors, and a working international collaboration are required to detect and to measure this elusive type of radiation.

And yet – just on account of their weak interaction – gravitational waves (just as neutrinos) can give us knowledge about cosmic events to which the electromagnetic window will be closed forever.

This goes for the processes in the (millisecond) moments of a supernova collapse, as well as of the many mergers of binaries that might be hidden by galactic dust. Such high-frequency events (a few Hz up to a few kHz) will be accessible from the detectors on Earth. For the signals to be significant, a number of ground-based detectors should be operated in coincidence, and only such joint analyses will allow to locate the source in the sky.

The perspective of detecting events with non-electromagnetic radiation also holds for the distant, but violent, mergers of galaxies and their central (super)massive black holes. The low frequencies (10^{-5} Hz to 1 Hz) characteristic of such sources are accessible only from space, e.g. with LISA. The expected high signal-to-noise ratios will allow unquestionable detection with only one detector, and will even allow to locate the source in a narrow region in the sky.

A LISA follow-on mission, but also combinations of terrestrial detectors, might probe the GW background from the very beginning of our universe (10^{-14} s or even only 10^{-22} s after the big bang).[48]

In this way, gravitational wave detection can be regarded as a new window to the universe, but to open this window we must continue on our way in building and perfecting our antennas. It will only be after these large interferometers are completed (and perhaps even only after the next generation of detectors) that we can reap the fruits of this enormous effort: a sensitivity that will allow us to look far beyond our own galaxy, perhaps to the very limits of the universe.

Recent understanding of the very violent events between colliding galaxies makes measurements at even lower frequencies than accessible for LISA a very desirable goal. With dimensions as envisaged for ASTROD one has improved chances of seeing such events in the light of gravitational waves. That could make ASTROD a logical extension of the – so far – much more progressed mission LISA.

References

1. A. Einstein, Sitzungsber. Preuss. Akad. Wiss., (1916) 688–696.
2. A. Einstein, Sitzungsber. Preuss. Akad. Wiss., (1918) 154–167.
3. K. Thorne, *Gravitational Radiation*, in: *300 Years of Gravitation*, ed. S.W. Hawking, W. Israel, Cambridge University Press (1987) 330–458.
4. K. Thorne, *Gravitational Radiation – A New Window Onto the Universe*, Rev. Mod. Astron. **10** (1997) 1–28.
5. A. Buonanno, T. Damour, *Effective one-body approach to general two-body dynamics*, Phys. Rev. D **59** (1999) 084006 1–24.
6. B.F. Schutz, *Lighthouses of gravitational wave astronomy – Prospects with LIGO and LISA*, in: *Lighthouses of the Universe*, M. Gilfanov, R. Sunyaev, E. Churakov, Eds., ESO Astrophysics Symposia, (2002) 207–224.
7. R. Weiss, *Electromagnetically coupled broadband gravitational antenna* in: *Quarterly Progress Report, Research Laboratory of Electronics*, MIT **105** (1972) 54–76.
8. D. Shoemaker et al., *Noise behavior of the Garching 30 meter prototype gravitational wave detector*, Phys. Rev. D **38** (1988) 423–432.
9. A. Abramovici et al., *LIGO: The Laser Interferometer Gravitational-Wave Observatory*, Science **256** (1992) 325–333.
10. A. Lazzarini, *The Status of LIGO*, in: *Gravitational Wave Detection II*, Universal Academy Press, Tokyo (2000) 1–13.
11. A. Vicere, *The VIRGO experiment*, in: AIP Conference Proc. **555**, AIP, (2001) 138–145.
12. A. Rüdiger and K. Danzmann, *The GEO 600 gravitational wave detector – status, research, development*, in *Gyros, clocks, interferometers: Testing relativistic gravity in space*, Lecture Notes in Physics **562** (2001) 131–140.
13. B. Willke and the GEO team, *The GEO 600 gravitational wave detector*, Class. Quantum Grav. **19** (2002) 1377–1387
14. B.J. Meers, *Recycling in laser-interferometric gravitational-wave detectors*, Phys. Rev. D **38** (1988) 2317–2326.
15. G. Heinzel et al., *Dual recycling for GEO 600*, Class. Quantum Grav. **19**, (2001) 1547–1553.
16. J. Mizuno et al., *Resonant sideband extraction: a new configuration for interferometric gravitational wave detectors*, Phys. Lett. A **175** (1993) 273–276.
17. M.K. Fujimoto, *Overview of the TAMA Project*, in: *Gravitational Wave Detection II*, Universal Academy Press (Tokyo, 2000) 41–43.
18. about 1000 hour run: `http://tamago.nao.ac.jp/tama/daq/recom/recom3/`
19. D.E. McClelland et al., *Second-generation laser interferometer for gravitational wave detection*, Class. Quantum Grav. **18** (2001) 4121–4126.
20. I. Zawischa et al., *The GEO 600 laser system*, Class. Quantum Grav. **19** (2002) 1775–1781.
21. A. Rüdiger et al., *A mode selector to suppress fluctuations in laser beam geometry*, Opt. Acta **28** (1981) 641–658.
22. V.B. Braginsky, M.L. Gorodetsky, S.P. Vyatchanin, *Thermodynamical fluctuations and photo-thermal shot noise in gravitational antennae*, Phys. Lett. A **264** (1999) 1–10.
23. Y.T. Liu, K.S. Thorne, *Thermoelastic noise and homogeneous thermal noise in finite sized gravitational wave test masses*, Phys. Rev. D **62** (2000) 122002 1–10.
24. D. Schnier et al., *Power recycling in the Garching 30-m prototype interferometer for gravitational-wave detection*, Phys. Lett. A **225** (1997) 210–216.
25. G. Heinzel et al., *An experimental demonstration of resonant sideband extraction for*

laser-interferometric gravitational wave detectors, Phys. Lett. A **217** (1996) 305–314.
26. *"Proposal for continuing LIGO Operations (FY 2002 - 2006): Research and Development"*, LIGO Laboratory document M000352-00-M (Dec 2000) 117–162.
27. K. Kuroda, *Large-scale cryogenic gravitational wave telescope and R&D*, Gravitational Wave Detection II, S. Kawamura, N. Mio, Eds., Universal Academy Press (2000) 45–50.
28. Albrecht Rüdiger, `ftp://ftp.rzg.mpg.de/pub/grav/geo/georep/euro.ps` (1999)
29. A. Buonanno and Y. Chen, *Optical noise correlations and beating the standard quantum limit in advanced gravitational wave detectors*, Class. Quantum Grav. **18** (2001) L95–L101.
30. M.V. Plissi et al., *Aspects of the suspension system for GEO 600*, Rev. Sci. Instrum. **69** (1998) 3055–3061.
31. V.B. Braginsky et al., *Isolation of test masses in the advanced laser interferometric gravitational-wave antennae*, Rev. Sci. Instrum. **65** (1994) 3771–3774.
32. LISA Pre-Phase A Report, 2nd edition, Max-Planck-Institut für Quantenoptik, Report 233 (July 1998); often referred to as PPA2.
33. LISA: System and Technology Study Report, ESA document ESA-SCI(2000)11, July 2000, revised as `ftp://ftp.rzg.mpg.de/pub/grav/lisa/sts/sts_1.05.pdf`
34. V. Josselin, M. Rodrigues, P. Touboul, *Inertial sensor concept for the gravity wave missions*, Acta Astronautica **49/2** (2001) 95–103.
35. A. Cavalleri et al., *Progress in the development of a position sensor for LISA drag-free control*, Class. Quantum Grav. **18** (2001) 4133–4144.
36. González, et al., *Field emission electrical propulsion: Experimental investigations on microthrust FEEP thrusters*, IECP–91–103.
37. M. Fehringer, F. Rüdenauer, and W. Steiger, *Space-proven Indium liquid metal field ion emitters for ion microthruster applications*, 33rd AIAA Joint Propulsion Conf., Seattle (1997), AIAA 97-3057.
38. Proceedings Third International LISA Symposium, Golm/Berlin, July 2000, Class. Quantum Grav. **18** (2001) 3965–4164.
39. W.-T. Ni, *ASTROD – an overview*, Int. J. Mod. Phys. **D11** (2002) 947.
40. W.-T. Ni ed., *Collection of papers on ASTROD Mission Concept Study*, Center for Gravitation and Cosmology, GP-118.
41. A.-C Liao, W.-T. Ni, J.-T. Shy, *Pico-watt and femto-watt weak-light phase locking*, Int. J. Mod. Phys. **D11** (2002) 1075.
42. R. Schilling, *Angular and frequency response of LISA*, Class. Quantum Grav. **14** (1997) 1513–1519.
43. G. Giampieri, R. Hellings, M. Tinto, J. Faller, *Algorithms for unequal-arm Michelson interferometers*, Opt. Comm. **123** (1996) 669–678.
44. M. Tinto, J.W. Armstrong, *Cancellation of laser phase noise in an unequal-arm interferometer detector of gravitational radiation*, Phys. Rev. D **59** (1999) 102003.
45. F.B. Estabrook, M. Tinto, J.W. Armstrong, *Time-delay analysis of LISA gravitational wave data: Elimination of Spacecraft motion effects*, Phys. Rev. D **62** (200) 042002.
46. M. Tinto et al., *Time-delay interferometry for LISA*, Phys. Rev. D (2002), in press.
47. S.L. Larson, R.W. Hellings, W.A. Hiscock, *Unequal-arm space-borne gravitational wave detectors*, Phys. Rev. D, (2002) in press.
48. B. Allen, *The stochastic gravity-wave background: sources and detection*, in: *Relativistic gravitation and gravitational radiation*, Cambridge University Press (1997) 373–417 (p. 381/382).